Antarctic Science 14 (4): 412–421 (2002) © Antarctic Science Ltd Printed in the UK DOI: 10.1017/S0954102002000214

Electron microprobe characterization of ash layers in sediments from the central Bransfield basin (Antarctic Peninsula): evidence for at least two volcanic sources

S. FRETZDORFF[1] and J.L. SMELLIE[2]

[1]*Institut für Geowissenschaften, University of Kiel, Olshausenstrasse 40, D-24118 Kiel, Germany*
[2]*British Antarctic Survey, NERC, High Cross, Madingley Road, Cambridge CB3 0ET, UK*

Abstract: Bransfield Strait, a narrow active rift with three submarine basins, separates the South Shetland Islands from northern Antarctic Peninsula. Volcanism in Bransfield Strait commenced prior to 0.75 Ma and continues, with recent subaerial eruptions at Deception, Bridgeman and Penguin islands, submarine hydrothermal activity and numerous young basaltic seamounts located along the rift axis. Gravity cores were collected from five locations within the central Bransfield basin. Diatomaceous mud interbedded with terrigenous detritus and discrete ash layers up to 10 cm thick are the commonest sediment types in all the cores. The major element compositions of glass shards within the ash layers are, apart from the uppermost layer, compositionally similar to pyroclastic units preserved on Deception Island, a young (< 0.75 Ma) active stratovolcano. The uppermost ash layer cannot be closely matched compositionally to any known source in the Antarctic–Scotia Sea–southern South America region. Its presence indicates that a volcanic centre other than Deception Island contributed ash to the Bransfield basin. Based on the shallow stratigraphical position of the compositionally distinctive ash layer, only a few decimetres beneath the seafloor, its source volcano was probably active in historical times (< few hundred years).

Received 14 January 2002, accepted 19 August 2002

Key words: ash layers, Bransfield Strait, Deception Island, geochemistry

Introduction

Ash layers in sediments and ice are widespread in the South Shetland Islands (Matthies *et al.* 1988, 1990, Yoon *et al.* 1994, Pallàs *et al.* 2001), northern Antarctic Peninsula (Björck *et al.* 1991a), South Orkney Islands (Hodgson *et al.* 1998) and Scotia Sea (Moreton & Smellie 1998). Deception Island, the largest and most active volcano in the Antarctic Peninsula region (e.g. Smellie 2001), has been identified as the most likely source of these ash layers (Björck *et al.* 1991a, Smellie 1999). Previous tephrochronology studies highlighted the importance of establishing an accurate mid-term (decades to centuries) chronology in a region where dating methods like the ^{14}C method may be ambiguous or impossible to apply (Björck *et al.* 1991b, Pallàs *et al.* 2001). A major use for ash layers is in establishing a consistent regional chronology. In this study we present major element compositions of individual glass shards from discrete ash layers in sediment cores from the central basin in Bransfield Strait, taken during the ANT XV/2 cruise (1997–98) of RV *Polarstern*, in order to:

1) extend the tephrostratigraphy in the northern Antarctic Peninsula region,

2) investigate the eruptive sources of the volcanic ashes,

3) correlate the ash layers with known pyroclastic units of the source volcano(es), and

4) estimate the age of the ash layers.

Geological setting and volcanic activity

Bransfield Strait is a young active rift basin (e.g. Lawver *et al.* 1995) situated between the Antarctic Peninsula and the South Shetland Islands (Fig. 1). It is about 400 km long and 80 km in width between longitudes 62°–54°W, and latitudes 61°–64°S. The South Shetland Islands and northern Antarctic Peninsula are part of a large Mesozoic to Cenozoic magmatic arc founded on pre-Mesozoic continental basement (e.g. Moyes & Hamer 1983). The opening of Bransfield Strait is probably related to passive subduction of the former Phoenix plate and roll-back at the South Shetland trench (Barker 1982, Lawver *et al.* 1995).

Bransfield Strait is divided into three bathymetric sub-basins (western, central and eastern), which are separated by large volcanic edifices at Deception and Bridgeman islands (Jeffers *et al.* 1991). Due to the lack of active arc volcanism and subduction, Bransfield Strait is regarded here as a marginal basin formed by intra-continental rifting, rather than a back-arc basin with seafloor spreading on oceanic crust (Barker & Austin 1994). The basin is volcanically and tectonically active with opening rates of 11 mm a^{-1} (Dietrich *et al.* 1998). Several subaerial and submarine volcanic edifices are situated along and parallel to the major rifting axis. Quaternary volcanic rocks form

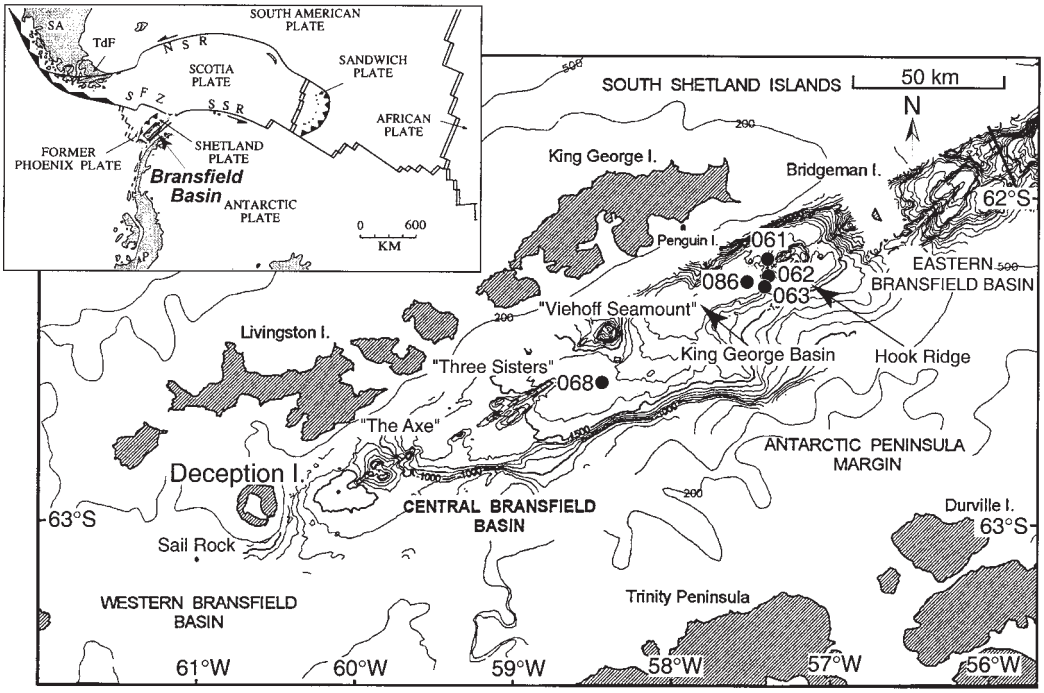

Fig. 1. Simplified bathymetric map of Bransfield Strait showing the locations of the sediment cores. Isobath contour interval is 100 m (redrawn after Gràcia *et al.* 1996).

Deception, Bridgeman and Penguin islands, several submarine volcanic seamounts and ridges in the central basin, and numerous small volcanic centres on Livingston, Greenwich and King George islands (Weaver *et al.* 1979, Smellie *et al.* 1984, Fisk 1990, Keller & Fisk 1992, Smellie *et al.* 1995, Gracia *et al.* 1996). The majority of the Quaternary volcanic rocks are basalts and rarer andesites, compositionally similar to other back-arc basin basalts (Keller *et al.* 1991). They are considered to record the transition from a subduction-driven to an initial seafloor spreading regime (Smellie *et al.* 1984, Smellie 1990, Lawver *et al.* 1995).

Deception Island is a young (< 0.75 Ma) stratovolcano situated on the north side of Bransfield Strait. It rises about 1.5 km above the sea floor and has a submerged basal diameter of 30 km with a central caldera (Fig. 1). The geology of the island is divided into pre- and post-caldera volcanic episodes, the Port Foster and Mount Pond groups, respectively (Smellie 2001). Major episodes of explosive activity occurred particularly during the syn- and post-caldera evolution of the island. It is seismically active and several small-volume eruptions occurred between 1967 and 1970 (Baker *et al.* 1975, Vila *et al.* 1992, Smellie 2002).

Four prominent submarine volcanic edifices are situated along a SW–NE orientation in the central Bransfield basin. They are "The Axe", "Three Sisters", "Viehoff Seamount" and Hook Ridge (Fig. 1). Between "Viehoff Seamount" and Hook Ridge there is a flat-bottomed, approximately 2000 m deep basin with a total sediment thickness of about 450 to 500 m (Guterch *et al.* 1985, Whiticar & Suess 1990). Yoon *et al.* (1994) studied the depositional environment of sediments in the so-called King George basin (i.e. that part of the central Bransfield basin opposite King George Island) and recognized Bouma sequences in several sediment cores. They were unable to correlate sediment units between cores, indicating a predominance of local sediment transport and depositional processes.

Sampling and analytical methods

During the ANT XV/2 cruise (in 1998) with RV *Polarstern*, gravity cores were obtained in two major areas: four closely spaced in the King George basin west of Hook Ridge, and one about 10 km west of "Viehoff Seamount" (Fig. 1, Table I). Core recovery ranged from 5.7 to 8.7 m. Sediment samples were taken every 5 cm. Following smear slide studies and macroscopic identification, samples with a high amount of glass particles were selected for further study. Because the locations of sediment cores PS47/061, 062 and 063 are very close (Fig. 1), only PS47/061 and the uppermost parts of PS47/063 were intensively studied. The samples were washed with distilled water to separate out the > 63 μm sediment fraction. More than 300 grains in each sample were counted for glass shards, crystals and lithics, to identify layers relatively rich in volcanic glass. In general, background values for glass in King George basin sediments are about 10% but reach about 40% in core PS47/068 (Fig. 2b). For each ash layer identified, glass particles were selected, embedded in resin and polished. Major element concentrations were measured on 20 fresh glass shards (i.e. without any optically visible signs of alteration, such as e.g. palagonite or Fe-hydroxide rims) using a Cameca SX50 electron microprobe (wavelength-dispersive spectrometer) at Geomar (Kiel, Germany), a

https://doi.org/10.1017/S0954102002000214 Published online by Cambridge University Press

Table I. Major element compositions (wt%) of ash layers in central Bransfield basin sediments.

Sediment depth	No.[a]	*A.–l.*[b]	SiO_2	TiO_2	Al_2O_3	FeO^t	MnO	MgO	CaO	Na_2O	K_2O	P_2O_5	Total
PS47/068: 62°34.86'S / 57°25.96'W; 1649m													
12 cm	12	*A*	56.25	2.25	14.26	9.32	0.21	2.94	5.90	4.65	1.10	0.42	97.30
			± 0.36	± 0.20	± 0.79	± 0.69	± 0.04	± 0.37	± 0.41	± 0.24	± 0.10	± 0.03	
45 cm	14	*B*	52.05	2.80	13.98	11.68	0.22	3.90	8.29	4.88	0.69	0.48	98.97
			± 0.57	± 0.04	± 0.23	± 0.46	± 0.05	± 0.27	± 0.28	± 0.22	± 0.05	± 0.05	
55 cm	6	*B*	52.36	2.83	13.98	11.09	0.19	3.44	8.29	4.49	0.63	0.46	97.76
			± 0.94	± 0.20	± 0.90	± 0.86	± 0.03	± 0.59	± 0.22	± 0.15	± 0.04	± 0.05	
80 cm	12	*C*	50.80	2.28	14.91	10.25	0.17	4.93	9.62	4.26	0.47	0.38	98.08
			± 0.52	± 0.14	± 0.49	± 0.68	± 0.03	± 0.54	± 0.39	± 0.21	± 0.02	± 0.05	
124 cm	19	*D*	52.92	2.93	14.03	11.81	0.23	3.85	6.99	4.41	0.77	0.58	98.54
			± 0.82	± 0.16	± 0.38	± 0.44	± 0.04	± 0.26	± 0.32	± 0.23	± 0.05	± 0.06	
160 cm	15	*E*	51.61	3.00	13.73	12.13	0.24	4.01	7.33	4.40	0.74	0.56	97.76
			± 0.78	± 0.12	± 0.35	± 0.28	± 0.04	± 0.33	± 0.19	± 0.16	± 0.07	± 0.07	
190 cm	12	*F*	52.99	3.14	13.55	11.98	0.23	3.71	7.07	4.32	0.78	0.59	98.36
			± 0.80	± 0.19	± 0.52	± 0.54	± 0.02	± 0.39	± 0.38	± 0.23	± 0.08	± 0.09	
230 cm	19	*G*	51.74	2.16	15.13	10.81	0.22	4.71	8.68	4.19	0.38	0.38	98.40
			± 0.56	± 0.10	± 0.38	± 0.37	± 0.03	± 0.13	± 0.14	± 0.11	± 0.03	± 0.04	
248 cm	19	*H*	53.08	2.03	15.34	10.10	0.22	4.15	7.95	4.38	0.45	0.43	98.12
			± 0.85	± 0.21	± 0.47	± 0.67	± 0.04	± 0.53	± 0.71	± 0.17	± 0.07	± 0.05	
[a]263 cm	10	*I*	51.37	2.14	15.00	10.64	0.23	4.65	8.47	4.34	0.39	0.40	97.61
			± 0.66	± 0.12	± 0.37	± 0.50	± 0.03	± 0.25	± 0.29	± 0.10	± 0.03	± 0.04	
[b]263 cm	7	*I*	70.69	0.44	14.77	3.38	0.16	0.31	0.95	5.12	2.27	0.11	98.20
			± 0.98	± 0.09	± 0.46	± 0.21	± 0.03	± 0.13	± 0.31	± 0.19	± 0.29	± 0.04	
280 cm	15	*J*	52.05	2.29	14.64	11.13	0.23	4.82	8.51	4.17	0.40	0.43	98.67
			± 0.55	± 0.17	± 0.41	± 0.48	± 0.03	± 0.38	± 0.54	± 0.16	± 0.05	± 0.04	
350 cm	19	*K*	53.65	1.77	15.61	8.85	0.20	5.10	8.65	4.07	0.66	0.39	98.94
			± 0.63	± 0.14	± 0.70	± 0.48	± 0.04	± 0.48	± 0.53	± 0.26	± 0.07	± 0.04	
376 cm	10	*L*	51.71	2.40	14.77	10.50	0.22	5.03	8.76	4.31	0.66	0.51	98.87
			± 0.98	± 0.26	± 0.55	± 0.55	± 0.04	± 0.52	± 0.31	± 0.22	± 0.06	± 0.05	
493 cm	7	*M*	53.22	2.69	14.32	11.36	0.23	3.88	7.35	4.53	0.81	0.51	98.89
			± 0.58	± 0.12	± 0.40	± 0.68	± 0.03	± 0.53	± 0.14	± 0.18	± 0.06	± 0.04	
PS47/061: 62°13.88'S / 57°28.74'W; 1934m													
41 cm	9	*No. 1*	60.91	0.89	16.47	5.81	0.14	3.30	6.50	4.16	1.22	0.24	99.65
			± 0.66	± 0.03	± 0.18	± 0.15	± 0.04	± 0.15	± 0.19	± 0.11	± 0.05	± 0.03	
45 cm	10	*No. 1*	59.38	0.93	16.10	6.36	0.15	3.08	6.50	4.30	1.21	0.08	98.09
			± 1.15	± 0.06	± 0.54	± 0.51	± 0.03	± 0.47	± 0.39	± 0.15	± 0.09	± 0.02	
242 cm	16	*No. 2*	55.70	1.82	15.56	9.37	0.18	3.40	7.04	4.04	0.83	0.37	98.30
			± 0.53	± 0.10	± 0.46	± 0.38	± 0.04	± 0.21	± 0.30	± 0.12	± 0.04	± 0.03	
[a]250 cm	10	*No. 2*	55.49	1.82	14.82	10.05	0.19	3.40	6.92	3.88	0.83	0.10	97.50
			± 1.12	± 0.11	± 0.42	± 0.28	± 0.03	± 0.22	± 0.24	± 0.16	± 0.07	± 0.02	
[b]250 cm	4	*No. 3*	52.42	1.34	15.26	9.20	0.20	5.52	9.71	3.49	0.62	0.09	97.86
			± 1.41	± 0.42	± 0.88	± 0.85	± 0.04	± 0.77	± 1.02	± 0.30	± 0.16	± 0.02	
255 cm	10	*No. 2*	54.75	1.86	14.71	9.87	0.21	3.46	7.30	3.80	0.87	0.11	96.92
			± 1.34	± 0.30	± 0.86	± 0.77	± 0.04	± 0.45	± 0.92	± 0.16	± 0.10	± 0.02	
418.5 cm	17	*No. 4*	53.64	2.77	14.97	11.32	0.22	4.08	7.53	4.00	0.71	0.55	99.80
			± 0.74	± 0.23	± 0.89	± 0.75	± 0.02	± 0.26	± 0.19	± 0.10	± 0.05	± 0.05	
515 cm	20		53.94	1.97	14.78	11.00	0.21	3.87	7.43	3.94	0.66	0.38	98.17
			± 0.76	± 0.06	± 0.26	± 0.14	± 0.02	± 0.09	± 0.09	± 0.04	± 0.03	± 0.04	
545 cm	17		54.87	1.79	15.71	9.82	0.19	3.83	7.20	3.93	0.89	0.39	98.63
			± 0.77	± 0.09	± 0.34	± 0.33	± 0.03	± 0.49	± 0.65	± 0.17	± 0.09	± 0.04	
PS47/063: 62°15.59'S / 57°28.22'W; 1994m													
24 cm	11	*No. 1*	60.19	0.91	15.93	5.70	0.15	3.26	6.15	4.34	1.32	0.25	98.21
			± 0.89	± 0.05	± 0.36	± 0.25	± 0.02	± 0.41	± 0.47	± 0.14	± 0.14	± 0.05	
219cm	14	*No. 2*	55.21	1.86	15.51	10.20	0.19	3.68	7.02	3.88	0.83	0.37	98.78
			± 0.64	± 0.13	± 0.66	± 0.48	± 0.03	± 0.19	± 0.27	± 0.06	± 0.09	± 0.03	
PS47/086: 62°16.81'S / 57°35.18'W; 2009m													
30 cm	6	*No. 1*	60.09	0.90	15.25	6.05	0.15	3.16	6.30	4.26	1.24	0.08	97.47
			± 1.50	± 0.04	± 0.39	± 0.31	± 0.03	± 0.33	± 0.40	± 0.14	± 0.08	± 0.03	

[a] No. of analysed glass shards with similar composition, [b] Capitals indicate individual ash-layers (A.-l.); numbers mark similar ash-layers found in the 3 neighbouring sediment cores, [c] Reference values are listed in Staudigel *et al.* (1999)

Table I continued opposite

https://doi.org/10.1017/S0954102002000214 Published online by Cambridge University Press

Table I. (concluded) Major element compositions (wt%) of ash layers in central Bransfield basin sediments.

Sediment depth	No.[a]	*A.–l.*[b]	SiO_2	TiO_2	Al_2O_3	FeO^t	MnO	MgO	CaO	Na_2O	K_2O	P_2O_5	Total
36 cm	10	*No. 1*	59.34	0.90	15.58	6.23	0.15	3.21	6.45	4.11	1.24	0.20	97.40
			± 1.48	± 0.06	± 0.31	± 0.27	± 0.03	± 0.30	± 0.44	± 0.13	± 0.11	± 0.03	
42 cm	11	*No. 1*	60.33	0.91	15.32	6.25	0.15	3.18	6.36	4.26	1.23	0.07	98.06
			± 0.93	± 0.07	± 0.41	± 0.28	± 0.03	± 0.36	± 0.39	± 0.15	± 0.08	± 0.02	
379.5 cm	6	*No. 2*	54.77	1.93	14.80	10.02	0.21	3.62	7.01	3.90	0.79	0.33	97.39
			± 0.56	± 0.33	± 0.54	± 0.56	± 0.03	± 0.33	± 0.15	± 0.23	± 0.05	± 0.08	
394 cm	6	*No. 2*	54.65	1.98	14.50	10.91	0.21	3.63	7.10	3.78	0.76	0.32	97.82
			± 0.64	± 0.14	± 0.51	± 0.59	± 0.03	± 0.17	± 0.17	± 0.10	± 0.09	± 0.04	
400 cm	7	*No. 3*	50.40	1.71	14.75	9.71	0.19	5.93	10.30	3.43	0.54	0.30	97.25
			± 1.10	± 0.41	± 0.69	± 0.78	± 0.03	± 0.41	± 1.05	± 0.41	± 0.04	± 0.04	
411 cm	6	*No. 3*	51.87	1.62	15.00	10.52	0.22	5.39	10.02	3.47	0.59	0.31	99.03
			± 0.48	± 0.05	± 0.28	± 0.31	± 0.02	± 0.15	± 0.19	± 0.06	± 0.02	± 0.04	
556 cm	11	*No. 4*	53.07	2.65	15.04	10.35	0.23	3.41	6.74	4.58	0.75	0.14	96.96
			± 0.90	± 0.14	± 0.48	± 0.48	± 0.04	± 0.30	± 0.40	± 0.19	± 0.12	± 0.03	
621.5 cm	11		56.21	2.38	14.53	9.57	0.22	3.26	5.84	4.38	0.92	0.59	97.90
			± 0.73	± 0.18	± 0.59	± 0.62	± 0.02	± 0.35	± 0.33	± 0.27	± 0.12	± 0.05	
Standards[c]													
JDF-D2	21		± 50.62	1.93	13.51	12.07	0.23	6.78	10.72	2.79	0.20	0.32	99.17
			± 0.70	± 0.05	± 0.33	± 0.13	± 0.02	± 0.21	± 0.14	± 0.05	± 0.02	± 0.05	

[a] No. of analysed glass shards with similar composition, [b] Capitals indicate individual ash-layers (A.-l.); numbers mark similar ash-layers found in the 3 neighbouring sediment cores, [c] Reference values are listed in Staudigel *et al.* (1999)

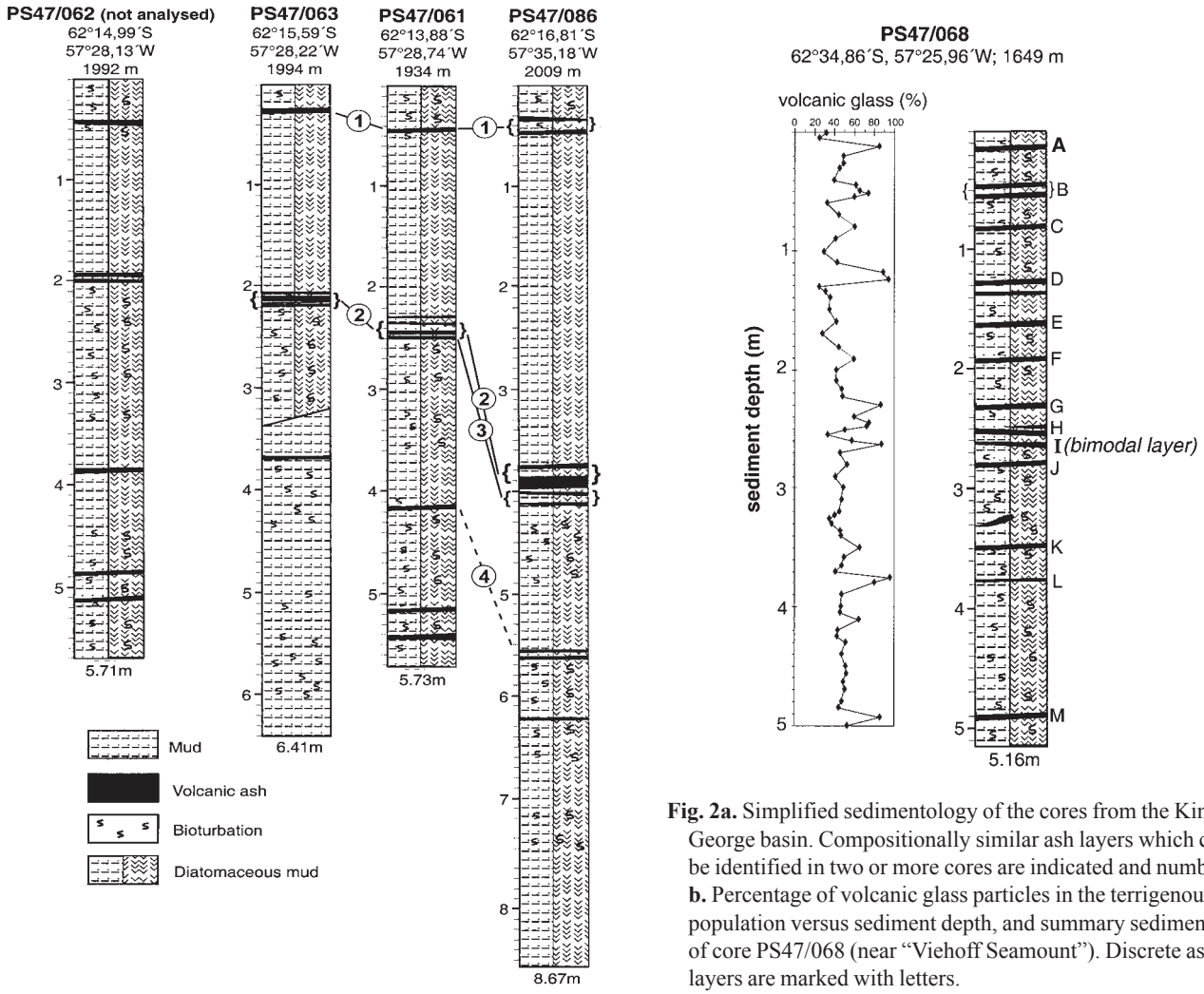

Fig. 2a. Simplified sedimentology of the cores from the King George basin. Compositionally similar ash layers which could be identified in two or more cores are indicated and numbered. **b.** Percentage of volcanic glass particles in the terrigenous grain population versus sediment depth, and summary sedimentology of core PS47/068 (near "Viehoff Seamount"). Discrete ash layers are marked with letters.

https://doi.org/10.1017/S0954102002000214 Published online by Cambridge University Press

beam current of 10 nA and accelerating voltage of 15 kV. The beam size was 10 µm wide to minimise Na loss, although Na loss was a problem in many samples and the relatively low totals support this analytical error. An international glass standard (JDF-D2; Table I) was measured after every 20 analyses to check precision, which is better than ± 0.7%. Ash layers containing at least 70% geochemically homogeneous glass shards were defined as distinct ash layers.

Results

Sediment petrography of the cores

Grey to very dark grey partly bioturbated diatomaceous mud of is the common sediment type in all cores (Fig. 2). The diatoms are typical for the Antarctic region (Abelmann & Gersonde 1991) and occur with sponge spicules. Terrigeneous detritus consists of volcanic glass, clay minerals, silt to fine sand-size feldspars, amphiboles and minor quartz. The sediment cores which were obtained west of Hook Ridge (hereafter collectively called King George basin cores) contain fine laminated turbiditic sequences of diatomaceous ooze lacking bioturbation (Fig. 2a), whereas there are no turbidite beds in core PS47/068 near "Viehoff Seamount" (Fig. 2b).

Volcanic glass morphology and composition

The average glass particle size is about 100 µm and the fraction consists mostly of light brown blocky fragments with a low vesicle content. Typical pumice particles and some elongate fragments of light brown glass also occur in the ash layers, together with subordinate nearly vesicle-free, blocky black shards. Some microcrystals, mainly plagioclase and opaque minerals, are present in the brown particles and are common in the black fragments.

Despite the high abundances of glass shards (40%) throughout core PS47/068, at least 13 ash layers with 60–100% glass were identified (Fig. 2b). The shards are brownish to black in colour. They are all basalts to basaltic andesites except for ash layer I at 263 cm below sea floor (cmbsf), which contains colourless and brown glass with bimodal basalt–rhyolite compositions (Table I, Fig. 3). By contrast, ash layers in the King George basin cores are more evolved, mainly basaltic andesites and andesites (Table I, Fig. 3). Based on the similar geochemical composition of the volcanic glass particles, four discrete ash layers were distinguished, each of which occurs in at least two cores (Fig. 2a). Ash layers No. 1 and 2 were identified in all of the cores. Ash layer No. 1 (20–50 cmbsf) consists entirely of colourless, silica-rich andesite glass shards, whereas ash layer No. 2 consists mainly of brown basaltic andesite glass particles (80% of the terrigenous fraction). The latter occurs at 200 cmbsf in cores 061 and 063, and 380 cmbsf in core 086. Ash layer No. 3 (brown basalt–basaltic andesite glass shards) was only identified in cores PS47/061 (at 250 cmbsf) and 086 (400 cmbsf). Its presence is suspected in core PS47/063, but it has probably been masked by extensive local bioturbation. Ash layer No. 4 also consists mainly of brown glass shards (70% of the terrigenous fraction) but with slightly more siliceous basaltic andesite compositions; it occurs at 415 and 560 cmbsf, in cores PS47/061 and 086, respectively (Fig. 2a).

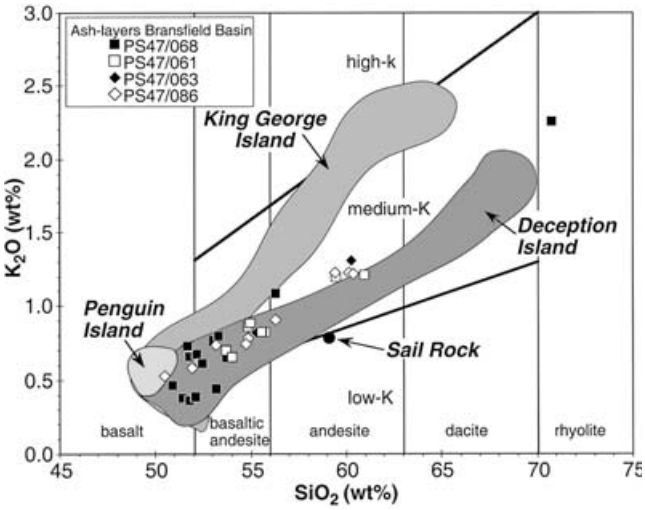

Fig. 3. K_2O vs SiO_2 content of individual ash layers identified in the four sediment cores compared with compositions of Deception Island lavas (data from Baker *et al.* 1975, Roobol 1979, Weaver *et al.* 1979, Tarney *et al.* 1982, Keller *et al.* 1991, Smellie *et al.* 1992, Smellie unpublished data), Penguin (Tarney *et al.* 1982, Keller *et al.* 1991) and King George islands (Fisk 1990, Saunders & Tarney 1984, Smellie *et al.* 1984), and Sail Rock (Keller *et al.* 1991). Classification fields are from Le Maitre (1989) and Peccerillo & Taylor (1976).

Surprisingly, no ash layers from the "Viehoff Seamount" core can be correlated compositionally with any at the King George basin sites.

Major element analyses of glass shards from the homogeneous ash layers are presented in Table I. The majority of the ash layers range from basalt to low-silica andesite and are medium-K tholeiites (Fig. 3). Glass fragments from ash layer I in core PS47/068 (near "Viehoff Seamount") have bimodal basalt and rhyolite compositions (Table I).

Discussion

Source of the ash layers

Apart from ash layer No. 1 (King George basin), all others plot within the geochemical field for Deception Island magmas and a Deception Island source seems likely (Fig. 3). However, Na_2O contents in several samples extend to significantly lower values and slightly higher SiO_2 and

https://doi.org/10.1017/S0954102002000214 Published online by Cambridge University Press

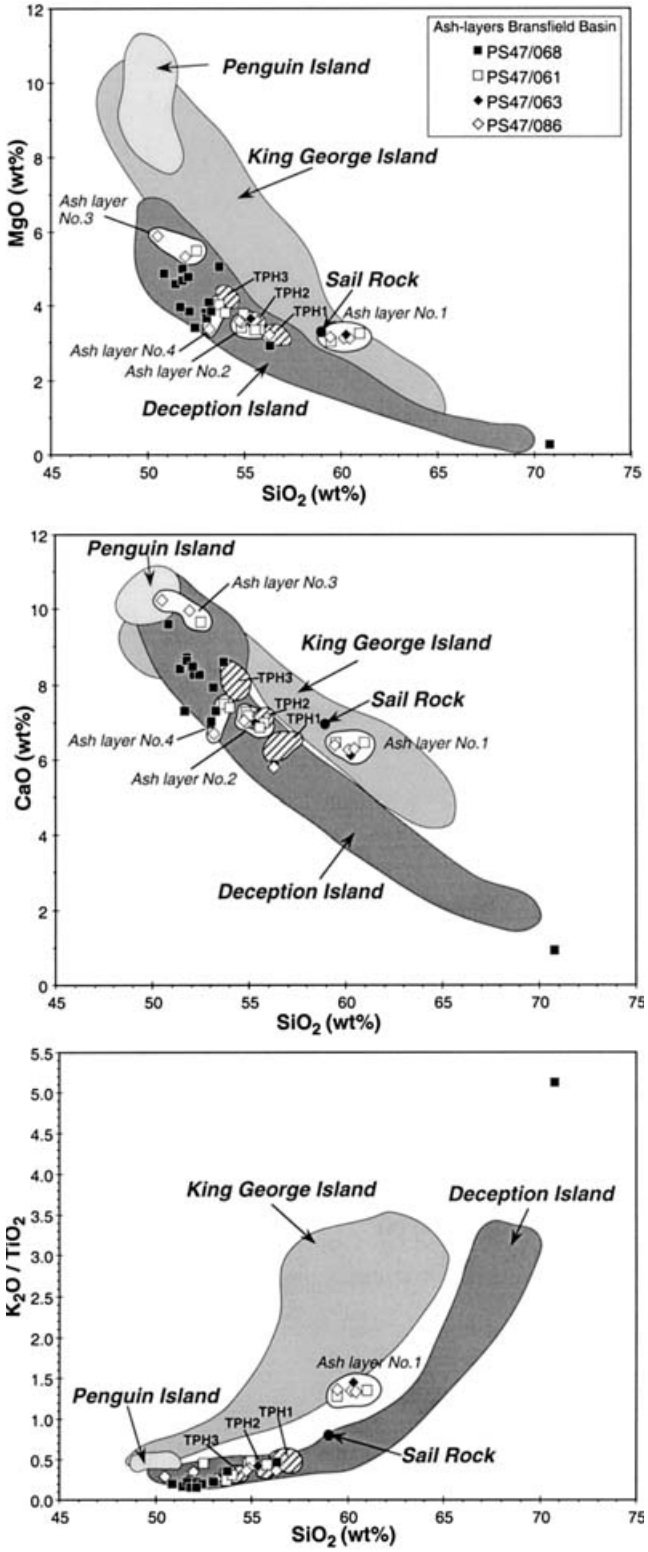

Fig. 4a. MgO, CaO, and K_2O/TiO_2 ratios versus SiO_2 contents of individual ash layers identified in the four sediment cores. For comparison, major element concentrations in volcanic rocks from Deception, Penguin and King George islands, Sail Rock and ice tephra layers on Livingston Island (TPH1–TPH3, Pallàs *et al.* 2001) are also shown. For data sources see Fig. 3.

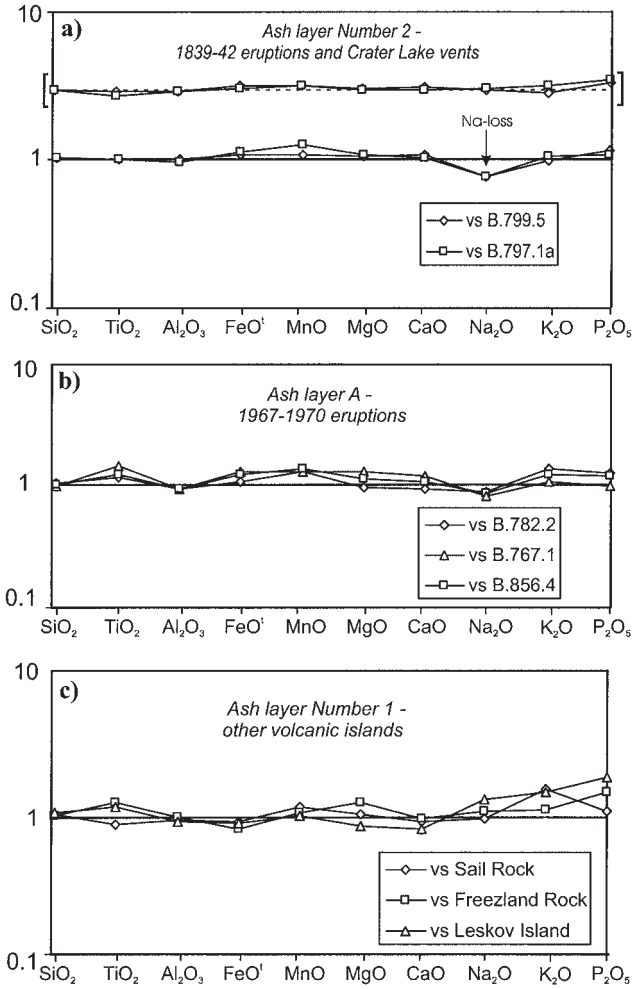

Fig. 5. Major element compositional comparisons between **a.** ash layer No. 2 (King George basin), 1839–1842 tephra (B.797.1a) and Crater Lake vents (B.799.5) on Deception Island, **b.** ash layer A (near Viehoff Seamount) and 1967–70 tephra on Deception Island, and **c.** ash layer No. 1 (King George basin) and andesites from Leskov Island and Freezland Rock (South Sandwich Islands) and Sail Rock. Analyses used in these comparisons are given in Table II. In each case, analyses of the marine ash layers from this study were divided by representative analyses from the sources indicated. A perfect compositional match would yield a horizontal line with a value of 1. In a, the effect of analytical Na-loss is obvious. When the analysis is recalculated to correct for Na-loss (upper data set, between parentheses), the compositional similarity to ashes from 1839–42 and pre-1829 eruptions on Deception Island is remarkable.

K_2O contents than are typical for Deception Island (Fig. 3, Table I). Bulk-sample compositions are known to be less siliceous than their corresponding glass shard fraction, depending on the nature and amounts of crystals, and alteration processes (e.g. Keller *et al.* 1978). Although comparisons were made with bulk-sample XRF analyses of

https://doi.org/10.1017/S0954102002000214 Published online by Cambridge University Press

Table II. Major element analyses (wt%) of lavas from Bransfield Strait and South Sandwich Islands, used in this paper for comparative purposes.

Sample	Location	SiO_2	TiO_2	Al_2O_3	FeO^T	MnO	MgO	CaO	Na_2O	K_2O	P_2O_5	Total
B.799.5	Deception Island (1839–42)[1]	55.75	1.86	15.83	8.83	0.17	3.33	6.76	5.37	0.87	0.33	99.10
B.797.1a	Deception Island (pre-1829, Crater Lake area)[1]	55.59	1.99	16.02	9.25	0.17	3.44	7.09	5.23	0.77	0.32	99.87
B.782.2	Deception Island (1967, less evolved)[1]	56.17	2.04	15.84	9.06	0.17	3.23	6.61	5.47	0.84	0.35	99.78
B.768.2	Deception Island (1967, evolved)[1]	61.13	1.36	16.02	6.88	0.17	1.91	4.44	6.38	1.19	0.47	99.95
B.767.1	Deception Island (1970)[1]	59.59	1.60	16.07	7.44	0.17	2.34	5.13	6.02	1.07	0.44	99.87
SR1	Sail Rock[2]	59.00	1.02	17.60	6.30	0.12	3.20	7.00	4.30	0.80	0.22	99.56
SSF.1-3	Freezland Rock[3]	59.85	0.70	16.68	7.11	0.13	2.61	6.67	3.81	1.08	0.16	98.80
SSL.4-2	Leskov Island[3]	57.76	0.76	17.74	6.51	0.14	3.86	7.98	3.20	0.83	0.13	98.91

Sources: [1] Unpublished data of J.L. Smellie, [2] Keller *et al.* 1991, [3] Pearce *et al.* 1995

Deception magmas, the disparities are unlikely to be due to the presence of phenocrysts in the Deception rocks. Basalts and basaltic andesites on the island are essentially aphyric, usually containing only a few microphenocrysts. Phenocrysts only become conspicuous in some andesites and dacites (unpublished information of JLS). The compositional differences may be a function of unsystematic Na-loss during microprobe analyses but in other respects the samples are similar to Deception Island magmas. We suggest that Deception Island is the most probable source, a conclusion also reached by others for submarine ash layers in Bransfield Strait (Matthies *et al.* 1988). Deception Island has been the major source of Quaternary ash layers throughout the northern Antarctic Peninsula–Scotia Sea region (Bjork *et al.* 1991a, Hodgson *et al.* 1998, Moreton & Smellie 1998, Pallàs *et al.* 2001, Smellie 2001). The predominance of basaltic compositions in ash layers near "Viehoff Seamount" is consistent with their more proximal position only 125 km north-east of Deception Island, whereas more evolved (and more highly explosive?) eruptions may have dispersed the ashes found in the King George basin sites, almost 200 km from Deception Island. Both basalt and basaltic andesite ashes are however common in the Scotia Sea (unpublished information of S. Moreton, British Antarctic Survey).

Pallàs *et al.* (2001) studied ash layers in the coastal ice caps of Livingston Island. Three groups were identified based on bulk sample compositions (TPH1, TPH2, TPH3). TPH2 correlates well with volcanic material from several pre-1829 co-eruptive centres at Crater Lake on Deception Island. Our ash layer No. 2, from the King George basin, is compositionally very similar to TPH2 and also to Deception Island ash erupted from 1839–42 vents near Crater Lake (Figs 4 & 5a; Table II). Moreover, when the analysis of ash layer No. 2 is normalized to the Na_2O content of the *in situ* Deception rocks, the compositional comparison is astonishingly good. However, like Pallas et al. (2001), we favour the pre-1829 centres as a source - they are prominent pyroclastic tuff cones and maar types, whereas the 1839–42 centres are much smaller cones formed during low energy Strombolian or Hawaiian eruptions and are unlikely to have dispersed ash far from the island (cf. Smellie 2001).

The uppermost ash layer (A) in core PS47/068 is compositionally similar to TPH1 of Pallàs *et al.* (2001), which those authors correlated with a 1970 Deception Island eruption. We find a slightly better correspondence for ash layer A with less evolved volcanic ash from the 1970 eruptions, but either comparison is weaker than for ash layer No. 2 and the pre 1829 centres, and we are not confident of the match for ash layer A (Fig. 5b). None of our other ash layers can be correlated quite so closely with specific analysed samples from Deception Island, either because the corresponding units on Deception Island were not analysed, or those units have been eroded or are covered by younger volcanic material. A similar problem of compositional matching with analogous units on Deception Island was noted by Pallàs *et al.* (2001) for their ash layer TPH3.

Moreton & Smellie (1998) identified a visually prominent and widespread bimodal ash layer in sediment cores from the Scotia Sea which compositionally resembles ash layer I in sediment core PS47/068. However, the Scotia Sea ash has been dated at about 10 ka in age (unpublished information of S. Moreton) whereas ash layer I in Bransfield Basin is likely to be much younger (hundreds of years? - see below). Deception Island has repeatedly erupted magmas with similar compositions at different times in its history (unpublished information of JLS) and correlations based solely on major oxide compositions should be treated with caution. Therefore, it is currently impossible to validate our compositional correlations with specific Deception Island tephras, although they are consistent with our assertion of a Deception Island source for the ash layers generally. The occurrence of a likely second, younger bimodal ash layer derived from Deception Island also indicates that bimodal eruptions have occurred on the island on more than one occasion, even though only one ash unit preserved on the island is known to be bimodal (the pre-caldera Outer Coast Tuff Formation; Smellie 2001).

Uniquely in the data set, ash layer No. 1 (King George basin) consistently plots well off Deception Island magmatic trends for most elements (i.e. lower Na_2O, TiO_2, Fe_2O_3 and P_2O_5, higher CaO, MgO, K_2O; Figs 3 & 4). The differences cannot simply be ascribed to problematical Na-loss, and Deception Island is therefore an unlikely source. There is also no compositional similarity with other subaerial centres in Bransfield Strait (Bridgeman Island,

https://doi.org/10.1017/S0954102002000214 Published online by Cambridge University Press

Penguin Island), and seamounts in Bransfield Strait are probably an unlikely source for explosive eruptions because of their depth (mainly > 1000 m). Despite a substantial similarity to lavas from the South Shetland Islands (especially King George Island), volcanic activity in the South Shetland Islands ceased at about 20 Ma apart from small widely scattered Quaternary tuff cones (Pankhurst & Smellie 1983, Smellie *et al.* 1995). The Quaternary tuff cone centres are the most primitive basalts in the South Shetland volcanic arc (Smellie *et al.* 1984). They are compositionally dissimilar to ash layer No. 1 and no correlation is possible. With its low K_2O and comparatively high Na_2O contents, ash layer No. 1 cannot be derived from any of the large alkaline centres in Marie Byrd Land (LeMasurier 1990), nor from the relatively potassic calc–alkaline centres of southern South America (Naranjo & Stern 1998). There is a broad similarity to some andesites in the active volcanoes in the South Sandwich Islands (Leskov Island, Freezland Rock; Pearce *et al.* 1995, Fig. 5c). However, the compositional match is relatively weak, because the South Sandwich Islands are situated 2000 km east-north-east of Bransfield Strait, in a direction contrary to current prevailing winds, and the ash layer is also relatively coarse grained for such a distant source (*c.* 0.5–3 mm). A better, but still relatively weak chemical match can be found with rocks from Sail Rock, a poorly known volcano 20 km south-west of Deception Island and preserved only as a tiny sea stack (Keller *et al.* 1991; Fig. 5c). The Sail Rock volcano was discovered only in March 1987 (British Antarctic Survey 1987, p. 88). Based on current knowledge there are no other subaerial sources known in the Bransfield Strait–northern Antarctic Peninsula–Scotia Arc region.

However, hydrothermal activity has recently been found on Hook Ridge (Bohrmann *et al.* 1999, Dählmann *et al.* 2001, Klinkhammer *et al.* 2001; Fig. 1). The volcanic edifice reaches a water depth of 1050 m and samples were taken directly from the crater which consisted of hot sediment (42–49°C) underlain by a thick ash layer (Klinkhammer *et al.* 2001). Although only very shallow submarine eruptions are known to produce ash deposits (e.g. Heiken *et al.* 1983) we have to consider that the source of ash layer No. 1 could also be Hook Ridge. There are no published analyses of ashes from Hook Ridge.

The age of ash layer No. 1 is likely to be very young. It occurs at a depth of only 60 cmbsf, in a setting where sedimentation rates are likely to be as high as 0.26–1 cm a^{-1} (Han 1988, Brault & Simoneit 1990). This suggests a minimum age for ash layer No. 1 of approximately 60–230 a, implying that the source volcano erupted in historical times.

Conclusions

Multiple ash layers were recovered in piston cores from Bransfield basin. They probably represent products of explosive eruptions on Deception Island, the most active subaerial volcano in the Antarctic Peninsula region. Most of the ash layers are basalts or basaltic andesites, but andesite and rhyolite compositions are also present. One layer (I in PS47/068) is compositionally bimodal (basalt–rhyolite), is much younger than another Deception-sourced bimodal ash layer found in Scotia Sea, and has no known counterpart on Deception volcano. These observations suggest that bimodal eruptions have occurred more than once on the island. A compositionally distinctive andesite ash layer (No. 1) is also identified which was not sourced in the Deception volcano. Its composition cannot be matched with any known volcano in Antarctica, southern South America and South Sandwich Islands. Whatever the source of ash layer No. 1 is, the position of the layer only a few decimetres below the seafloor suggests that the source volcano was recently active (< few hundred years).

Acknowledgements

We thank Gerhard Borhmann, Anke Dählmann, Jens Greinert, Teal Riley, Markus Schumann and the captain and crew of the *Polarstern* for able assistance with the sampling at sea. G. Bohrmann and J. Greinert are also thanked for providing the sediment core descriptions (Fig. 2). Many thanks to A. Dählmann for fruitful discussions and corrections of a former version, Stefanie Haus and Markus Zimmerer for their extensive help during sample preparation and Otto Schneider for his assistance during the electron microprobe analyses. W. LeMasurier and P. Kyle provided constructive comments on the paper.

References

Abelmann, A. & Gersonde, R. 1991. Biosiliceous particle flux in the Southern Ocean. *Marine Chemistry*, **35**, 503–536.

Baker, P.E., McReath, I., Harvey, M.R., Roobol, M.J. & Davies, T.G. 1975. The geology of the South Shetland Islands: V. Volcanic evolution of Deception Island. *British Antarctic Survey Scientific Reports,* No. 78, 79 pp.

Barker, D.H.N. & Austin, J.A. 1994. Crustal diapirism in Bransfield Strait, West Antarctica: evidence for distributed extension in marginal-basin formation. *Geology,* **22**, 657–660.

Barker, P.F. 1982. The Cenozoic subduction history of the Pacific margin of the Antarctic Peninsula: ridge crest-trench interactions. *Journal of the Geological Society of London,* **139**, 787–801.

Björck, S., Sandgren, P. & Zale, R. 1991a. Late Holocene tephrochronology of the Northern Antarctic Peninsula. *Quaternary Research*, **36**, 322–328.

Björck, S., Hjort, C., Ingólfsson, O. & Skog, G. 1991b. Radiocarbon dates from the Antarctic Peninsula - problems and potential. *Quaternary Proceedings*, **1**, 55–65.

Bohrmann, G., Chin, C., Petersen, S., Sahling, H., Schwarz-Schampera, U., Greinert, J., Lammers, S., Rehder, G., Dählmann, A., Wallmann, K., Dijkstra, S. & Schenke, H.-W. 1999. Hydrothermal activity at Hook Ridge in the Central Bransfield Basin, Antarctica. *Geo-Marine Letters*, **18**, 277–284.

Brault, M. & Simoneit, B.R.T. 1990. Mild hydrothermal alteration of immature organic matter in sediments from the Bransfield Strait, Antarctica. *Applied Geochemistry*, **5**, 149–158.

British Antarctic Survey 1987. *British Antarctic Survey report for 1986/87*. Swindon: Natural Environment Research Council, 123 pp.

Dählmann, A., Wallmann, K., Sahling, H., Sarthou, G., Bohrmann, G., Petersen, S., Chin, C.S. & Klinkhammer, G.P. 2001. Hot vents in an ice-cold ocean: indications for phase separation at the southernmost area of hydrothermal activity, Bransfield Strait, Antarctica. *Earth and Planetary Science Letters,* **193**, 381–394.

Dietrich, R., Dach, R., Engelhardt, G., Kutterer, H., Lidner, K., Mayer, M., Menge, F., Mikolaiski, H.W., Niemeier, W., Orths, A., Perlt, J., Pohl, M., Salbach, H., Schenke, H.-W., Schöne, T., Seeber, G. & Soltau, G. 1998. GAP: Ein geodatisches Antarktisprojekt zur Lösung geodynamischer Aufgabenstellungen. *Zeitschrift für Vermessungskunde,* **2**, 49–60.

Fisk, M.R. 1990. Volcanism in the Bransfield Strait, Antarctica. *Journal of South American Earth Sciences,* **3**, 91–101.

Gràcia, E., Canals, M., Farran, M., Prieto, M.J., Sorribas, J. & the GEBRA Team 1996. Morphostructure and evolution of the Central and Eastern Bransfield Basins (NW Antarctic Peninsula). *Marine Geophysical Research,* **18**, 429–448.

Guterch, A., Grad, M., Janik, T., Perchuc, E. & Pajchel, J. 1985. Seismic studies of the crustal structure in west Antarctica 1979–1980: preliminary results. *Tectonophysics,* **114**, 411–429.

Han, M.W. 1988. Dynamics and chemistry of pore water fluids in marine sediments of different tectonic settings: Oregon Subduction Zone and Bransfield Strait extensional basin. *PhD thesis*, Oregon State University, Corvallis, 237 pp.

Heiken, G., Wohletz, K.H. & McCoy jr, F. 1983. Phreatomagmatic ash deposits associated with caldera collapse in a shallow submarine environment. *Eos, Transactions,* **64**, 876.

Hodgson, D.A., Dyson, C.L., Jones, V.J. & Smellie, J.L. 1998. Tephra analysis of sediments from Midge Lake (South Shetland Islands) and Sombre Lake (South Orkney Islands), Antarctica. *Antarctic Science,* **10**, 13–20.

Jeffers, J.D., Anderson, J.B. & Lawver, L.A. 1991. Evolution of the Bransfield basin, Antarctic Peninsula. *In* Thomson, M.R.A., Crame, J.A. & Thomson, J.W., *eds*. *Geological evolution of Antarctica.* Cambridge: Cambridge University Press, 481–485.

Keller, J., Ryan, W.B.F., Ninkowich, D. & Altherr, R. 1978. Explosive volcanic activity in the Mediterranean over the past 200,000 yr as recorded in deep-sea sediments. *Geological Society of American Bulletin,* **89**, 591–604.

Keller, R.A. & Fisk, M.R. 1992. Quarternary marginal basin volcanism in the Bransfield Strait as a modern analogue of the southern Chilean ophiolites. *In* Parson, L.M., Murton, B.J. & Browning, P., *eds. Ophiolites and their modern oceanic analogues.* Geological Society Special Publication, No. 60, 155–169.

Keller, R.A., Fisk, M.R., White, W.M. & Birkenmajer, K. 1991. Isotopic and trace element constraints on mixing and melting models of marginal basin volcanism, Bransfield Strait, Antarctica. *Earth and Planetary Science Letters,* **111**, 287–303.

Klinkhammer, G.P., Chin, C.S., Keller, R.A., Dählmann, A., Sahling, H., Sarthou, G., Petersen, S., Smith, F. & Wilson, C. 2001. Discovery of new hydrothermal vent sites in Bransfield Strait, Antarctica. *Earth and Planetary Science Letters,* **193**, 395–407.

Lawver, L.A., Keller, R.A., Fisk, M.R. & Strelin, J.A. 1995. Bransfield Strait, Antarctic Peninsula: active extension behind a dead arc. *In* Taylor, B., *ed. Backarc basins: tectonics and magmatism.* New York: Plenum Press, 315–342.

Le Maitre, R.W. 1989. *A classification of igneous rocks and glossary of terms: recommendations of the International Union of Geological Sciences Subcommision on the systematics of igneous rocks.* Oxford: Blackwell, 193 pp.

LeMasurier, W.E. 1990. Marie Byrd Land. *Antarctic Research Series,* **48**, 147–163.

Matthies, D., Mäusbacher, R. & Storzer, D. 1990. Deception Island tephra: a stratigraphical marker for limnic and marine sediments in Bransfield Strait area, Antarctica. *Zentralblatt für Geologie und Paläontologie,* **1**, 153–165.

Matthies, D., Storzer, D. & Troll, G. 1988. Volcanic ashes in Bransfield Strait sediments: geochemical and stratigraphical investigations (Antarctica). *In* Konta, J., *ed. Proceedings of the 2nd international conference on natural glasses*. Praha: Charles University, 139–147.

Moreton, S. & Smellie, J.L. 1998. Identification and correlation of distal tephra layers in deep sea sediment cores, Scotia Sea, Antarctica. *Annals of Glaciology,* **27**, 285–289.

Moyes, A.B. & Hamer, R.D. 1983. Contrasting origins and implications of garnet in rocks of the Antarctic Peninsula. *In* Oliver, P.R., James, P.R. & Jago, J.B., *eds*. *Antarctic Earth Sciences*. Canberra: Australian Academy of Science, 358–362.

Naranjo, J.A. & Stern, C.R. 1998. Holocene explosive activity of Hudson volcano, southern Andes. *Bulletin of Volcanology,* **59**, 291–306.

Pallàs, R., Smellie, J.L., Casas, J.M. & Calvet, J. 2001. Using tephrochronology to date temperature ice: correlation between ice tephras on Livingston Island and eruptive units on Deception Island volcano (South Shetland Islands, Antarctica). *The Holocene,* **11**, 149–160.

Pankhurst, R.J. & Smellie, J.L. 1983. K–Ar geochronology of the South Shetland Islands, Lesser Antarctica: apparent migration of Jurassic to Quaternary island arc volcanism. *Earth and Planetary Science Letters,* **66**, 214–222.

Pearce, J.A., Baker, P.E., Harvey, P.K. & Luff, I.W. 1995. Geochemical evidence for subduction fluxes, mantle melting and fractional crystallization beneath the South Sandwich Islands. *Journal of Petrology,* **36**, 1073–1109.

Peccerillo, A. & Taylor, S.R. 1976. Geochemistry of Eocene calc–alkaline volcanic rocks from the Kastamonu area, northern Turkey. *Contributions to Mineralogy and Petrology,* **58**, 63–81.

Roobol, M.J.A. 1979. A model for the eruptive mechanism of Deception Island from 1820 to 1970. *British Antarctic Survey Bulletin*, No. 49, 137–156.

Saunders, A.D. & Tarney, J. 1984. Geochemical characteristics of basaltic volcanism within back-arc basins. *In* Kokelaar, B.P. & Howells, M.F., *eds. Marginal basin geology: volcanic and associated sedimentary and tectonic processes in modern and ancient marginal basins.* Geological Society, Special Publication, No. 16, 59–76.

Smellie, J.L. 1990. Graham Land and South Shetland Islands. *Antarctic Research Series,* **48**, 302–359.

Smellie, J.L. 1999. The upper Cenozoic tephra record in the south polar region: a review. *Global and Planetary Change,* **21**, 51–70.

Smellie, J.L. 2001. Lithostratigraphy and volcanic evolution of Deception Island, South Shetland Islands. *Antarctic Science,* **13**, 188–209.

Smellie, J.L. In press. The 1969 subglacial eruption on Deception Island (Antarctica): events and processes during an eruption beneath a thin glacier and implications for volcanic hazards. *In* Smellie, J.L. & Chapman, M.G., *eds. Volcano-ice interaction on Earth and Mars.* Geological Society Special Publication, No. 202.

Smellie, J.L., Hofstetter, A. & Troll, G. 1992. Fluorine and boron geochemistry of an ensialic mariginal basin volcano: Deception Island, Bransfield Strait, Antarctica. *Journal of Volcanology and Geothermal Research,* **49**, 255–267.

Smellie, J.L., Liesa, M., Munoz, J.A., Sàbat, F., Pallàs, R. & Willam, R.C.R. 1995. Lithostratigraphy of volcanic and sedimentary sequences in central Livingston Island, South Shetland Islands. *Antarctic Science,* **7**, 99–113.

SMELLIE, J.L., PANKHURST, R.J., THOMSON, M.R.A. & DAVIES, R.E.S. 1984. The geology of the South Shetland Islands. VI. Stratigraphy, geochemistry and evolution. *British Antarctic Survey Scientific Reports,* No. 87, 85 pp.

STAUDIGEL, H., TAUXE, L., GEE, J.S., BOGAARD, P., HASPELS, J., KALE, G., KALE, A., LEENDERS, A., MEIJER, P., SWAAK, B., TUIN, M., VAN SOEST, M.C., VERDUMEN, E.A.TH. & ZEVENHUIZEN, A. 1999. Geochemistry and Intrusive directions in sheeted dikes in the Troodos Ophiolite: implications for mid-ocean ridge spreading centers. *Geochemistry, Geophysics, Geosystems,* **1**, 1999GC000001.

TARNEY, J., WEAVER, S.D., SAUNDERS, A.D., PANKHURST, R.J. & BARKER, P.F. 1982. Volcanic evolution of the northern Antarctic Peninsula and the Scotia arc. *In* THORPE, R.S., *ed. Andesites*. Chichester: John Wiley, 371–413.

VILA, J., ORTIZ, R., CORREIG, A.M. & GARCIA, A. 1992. Seismic activity on Deception Island. *In* YOSHIDA, Y., KAMINUMA, K. & SHIRAISHI, K., *eds. Recent progress in Antarctic earth science*. Tokyo: Terra Scientific Publishing Company, 449–456.

WEAVER, S.D., SAUNDERS, A.D., PANKHURST, R.J. & TARNEY J. 1979. A geochemical study of magmatism associated with the initial stages of back-arc spreading: the Quaternary volcanics of Bransfield Strait from South Shetland Islands. *Contributions to Mineralogy and Petrology,* **68**, 151–169.

WHITICAR, M.J. & SUESS, E. 1990. Hydrothermal hydrocarbon gases in the sediments of the King George Basin, Bransfield Strait, Antarctica. *Applied Geochemistry,* **5**, 135–147.

YOON, H.I., HAN, M.W., PARK, B.K., OH, J.K. & CHANG, S.K. 1994. Depositional environment of near-surface sediments, King George Basin, Bransfield Strait, Antarctica. *Geo-Marine Letters,* **14**, 1–9.

https://doi.org/10.1017/S0954102002000214 Published online by Cambridge University Press